

Validity of the linear coupling approximation in heavy-ion fusion reactions at sub-barrier energies

K. Hagino* and N. Takigawa

Department of Physics, Tohoku University, Sendai 980-77, Japan

M. Dasgupta, D. J. Hinde, and J. R. Leigh

Department of Nuclear Physics, Research School of Physical Sciences and Engineering, Australian National University, Canberra, ACT 0200, Australia

(Received 26 July 1996)

The role of higher order coupling of surface vibrations to the relative motion in heavy-ion fusion reactions at near-barrier energies is investigated. The coupled channels equations are solved to all orders and also in the linear and the quadratic coupling approximations. Taking $^{64}\text{Ni} + ^{92,96}\text{Zr}$ reactions as examples, it is shown that all order couplings lead to considerably improved agreement with the experimentally measured fusion cross sections and average angular momenta of the compound nucleus for such heavy, nearly symmetric systems. The importance of higher order coupling is also examined for asymmetric systems like $^{16}\text{O} + ^{112}\text{Cd}$, ^{144}Sm , for which previous calculations of the fusion cross section seemed to indicate that the linear coupling approximation was adequate. It is shown that the shape of the barrier distributions and the energy dependence of the average angular momentum can change significantly when the higher order couplings are included, even for systems where measured fusion cross sections may seem to be well reproduced by the linear coupling approximation. [S0556-2813(97)00201-X]

PACS number(s): 25.70.Jj, 24.10.Eq, 21.60.Ev, 27.60.+j

I. INTRODUCTION

The analysis of the fusion process in terms of the barrier distribution has generated renewed interest in heavy-ion collisions at energies below and near the Coulomb barrier [1–11]. Early studies of sub-barrier fusion reactions compared data and theory in terms of the excitation function of the fusion cross section. It is now well established that fusion cross sections at sub-barrier energies may be enhanced by several orders of magnitude compared with predictions of a one-dimensional potential model, which is due to coupling of the relative motion to nuclear intrinsic degrees of freedom [12]. It has been shown that under the eigenchannel approximation, these couplings give rise to a distribution of potential barriers. Recently, Rowley, Satchler, and Stelson proposed a method to extract the barrier distribution directly from measured fusion cross sections [1]. Although, strictly speaking, this method has a clear physical meaning only in the limit of sudden tunneling, i.e., in the limit of a degenerate spectrum of intrinsic motions [13], the same analysis was later applied also to the case where the intrinsic motions have finite excitation energies [14]. The excitation function of the fusion cross section has to be measured with extremely high precision at small energy intervals in order to deduce meaningful barrier distributions. Such data are now available for several systems, and have shown that the barrier distribution is very sensitive to the nuclear structure of the colliding nuclei. The analysis of the barrier distribution clearly shows the effects of couplings to static deformations [2–4,6], vibrational degrees of freedom [5,6], transfer channels [5,6], and multiphonon states [7,8], as well as the effects of projectile ex-

citations [9], in a way much more apparent than in the fusion excitation function itself.

Another quantity which has recently received increasing attention in the study of heavy-ion sub-barrier fusion reactions is the angular momentum distribution of the compound nucleus [15–23]. As in the case of the fusion cross section, the angular momentum distribution is also affected by the coupling between the relative motion and intrinsic degrees of freedom. Experimental data show that the average angular momentum of the compound nucleus formed in heavy-ion fusion reactions at sub-barrier energies is systematically larger than the value expected using the one-dimensional potential model [15]. Furthermore, it has been pointed out that the angular momentum distribution is also sensitive to the details of the coupling [19].

The fusion barrier distribution, the angular momentum distributions, and the fusion excitation function all reflect the physical processes occurring in fusion. In comparing measurement and calculation, the excitation function shows most sensitively the energy of the lowest barrier, while the others show more clearly the effect of couplings over the whole range of the barrier distribution. Therefore a simultaneous presentation of the data and theory in all three forms (if possible) allows the most complete comparison of data and theory.

Theoretically the standard way to address the effects of the coupling between the relative motion and the intrinsic degrees of freedom is to solve the coupled channels equations, including all the relevant channels. Most of the coupled channels calculations performed so far use the linear coupling approximation, where the coupling potential is expanded in powers of the deformation parameter, keeping only the linear term. While this approach reproduces the experimental data of fusion cross sections for very asymmetric systems, it does not explain the data for heavier and nearly

*Electronic address: hagino@nucl.phys.tohoku.ac.jp

symmetric systems [15,17,21–23]. Thus, it is of interest to examine the validity of one of the main approximations in these calculations, namely, the linear coupling approximation, and see whether the effects of nonlinear coupling improve the agreement between data and the theoretical calculations for such systems. Even in asymmetric systems, the nonlinear couplings might be important to reproduce precisely measured data.

The effects of nonlinear coupling can be easily studied if the excitation energy of the intrinsic motion is very small so as to allow one to use the sudden tunneling approximation [13]. The experimental data of the excitation function of the fusion cross section as well as the barrier distribution for the $^{16}\text{O} + ^{154}\text{Sm}$, ^{186}W reactions were analyzed in this manner [4,6]. The effects of higher order couplings on barrier distributions in the limit of zero excitation energy has been discussed by Balantekin, Bennett, and Kuyucak in the framework of the interacting boson model (IBM) [24]. However, for nuclear surface vibrations the excitation energies cannot be neglected in most cases, and one has to solve full coupled channels equations. Because of the complexity of such calculations, very few studies have addressed the effects of the higher order couplings for the vibrational motion. Esbensen and Landowne expanded the coupling potential up to the second order with respect to the deformation parameter, and have shown that second order coupling leads to a better agreement between the theoretical calculations and the experimental fusion cross sections for reactions between different nickel isotopes [25]. The quadratic coupling approximation was applied also to the $^{58,64}\text{Ni} + ^{92,100}\text{Mo}$ reactions [20]. There it was shown that the experimental data of both the fusion cross sections and the angular momentum distributions are well reproduced by the coupled channels calculations in the quadratic coupling approximation. Coupled channels calculations including full order coupling and the finite excitation energy of nuclear surface vibrations have recently been performed for the $^{58}\text{Ni} + ^{60}\text{Ni}$ reaction [7,26]. It is seen that higher order couplings are essential in reproducing the experimental data for this system, and the shape of the barrier distribution changes drastically when the effects of the higher order couplings are taken into account. References [7,26] do not, however, discuss the quality of the quadratic coupling approximation and the convergence of the expansion of the coupling potential.

Although all the above studies and the multidimensional tunneling model in Ref. [27] show the effects of higher order couplings in specific systems, there has not been any systematic effort to identify their degree of importance for different systems. Furthermore, it is not obvious whether calculations to all orders are necessary or an expansion up to the second order is sufficient. In view of the high precision data that have recently become available, a critical examination of the effects of these approximations on the cross sections and barrier distribution is necessary before making quantitative comparisons with experimental data.

In this paper we solve the coupled channels equations including the finite excitation energies of the vibrational states, and without introducing the expansion with respect to deformation parameters. The results of these calculations for fusion cross sections, average angular momenta, and barrier distributions are compared with those using the linear and

the quadratic coupling approximations. The paper is organized as follows. In Sec. II the coupled channels calculations which include higher order couplings are formulated. Explicit expressions for the matrix elements of higher order terms in both the nuclear and the Coulomb couplings are presented. It is seen that inclusion of up to the first order term in the Coulomb coupling is sufficient, but higher order terms are necessary for nuclear coupling. In Sec. III the coupled channels equations are solved for the $^{64}\text{Ni} + ^{92,96}\text{Zr}$ systems, where the experimental data of both the fusion cross sections and the average angular momenta of the compound nucleus are available. The asymmetric systems $^{16}\text{O} + ^{112}\text{Cd}$, ^{144}Sm are also studied in this section and the calculations are compared with measured fusion cross sections, barrier distributions, and the average angular momenta of the compound nucleus. The summary is given in Sec. IV.

II. COUPLED CHANNELS EQUATIONS AND COUPLING FORM FACTORS

Consider the problem where the relative motion between colliding nuclei couples to a vibrational mode of excitation of the target nucleus. For simplicity excitations of the projectile are not considered in this section. It is straightforward to extend the formulas to the case where many different vibrational modes are present and where projectile excitations also occur. For heavy-ion fusion reactions, to a good approximation one can replace the angular momentum of the relative motion in each channel by the total angular momentum J [28,29]. This approximation, often referred to as the no-Coriolis approximation, will be used throughout this paper. The coupled channels equations then read

$$\left[-\frac{\hbar^2}{2\mu} \frac{d^2}{dr^2} + \frac{J(J+1)\hbar^2}{2\mu r^2} + V_N(r) + \frac{Z_P Z_T e^2}{r} + n\hbar\omega - E_{\text{c.m.}} \right] \times \psi_n(r) + \sum_m V_{nm}(r) \psi_m(r) = 0, \quad (1)$$

where r is the radial component of the coordinate of the relative motion, μ the reduced mass, and V_N the nuclear potential in the entrance channel, respectively. $E_{\text{c.m.}}$ is the bombarding energy in the center-of-mass frame and $\hbar\omega$ is the excitation energy of the vibrational phonon. V_{nm} are the coupling form factors, which in the collective model consist of Coulomb and nuclear components. These two components are discussed in the following subsections.

A. Coulomb coupling form factors

We first consider the effects of higher order terms of the Coulomb component. In Refs. [24,25] it has been reported that the higher order Coulomb couplings are not important in heavy-ion fusion reactions. However, Ref. [25] studied only the excitation function of the fusion cross section, and did not discuss the barrier distribution. On the other hand, Ref. [24] ignored the finite excitation energy of nuclear intrinsic motions, though it discusses the effects on barrier distribution. Here we investigate the effects of higher order Coulomb couplings on both the excitation function of the fusion cross section and the barrier distribution and do not ignore the energy of nuclear intrinsic excitations. Initially, we con-

sider the case where the target has only a single phonon excitation.

The Coulomb potential between the spherical projectile and the vibrational target is given by

$$V_C(r) = \int d\mathbf{r}' \frac{Z_P Z_T e^2}{|\mathbf{r} - \mathbf{r}'|} \rho_T(\mathbf{r}') \Big|_{\hat{\mathbf{r}}=0} \\ = \frac{Z_P Z_T e^2}{r} + \sum_{\lambda' \neq 0} \frac{4\pi Z_P e}{2\lambda' + 1} \sqrt{\frac{2\lambda' + 1}{4\pi}} Q_{\lambda'0} \frac{1}{r^{\lambda'+1}}, \quad (2)$$

where ρ_T is the charge density of the target nucleus and $Q_{\lambda'0}$ the electric multipole operator defined as

$$Q_{\lambda'0} = \int d\mathbf{r} Z_T e \rho_T(\mathbf{r}) r^{\lambda'} Y_{\lambda'0}(\hat{\mathbf{r}}). \quad (3)$$

Equation (2) uses the fact that the angular momentum for the relative motion does not change in the no-Coriolis approximation, and that the associated spherical harmonics are evaluated at the forward angle $\hat{\mathbf{r}}=0$, leading to the factor $\sqrt{(2\lambda'+1)/4\pi}$. If we assume a sharp matter distribution for the target nucleus and a phonon excitation of multipolarity λ , then the electric multipole operator is given by [30]

$$Q_{\lambda'0} = \frac{3e}{4\pi} Z_T (R_T^{(0)})^{\lambda'} \\ \times \left\{ \alpha_{\lambda 0} \delta_{\lambda, \lambda'} + (-)^{\lambda'} \frac{(\lambda'+2)(2\lambda+1)}{2\sqrt{4\pi}} \right. \\ \left. \times \begin{pmatrix} \lambda & \lambda & \lambda' \\ 0 & 0 & 0 \end{pmatrix} (\alpha_\lambda \alpha_\lambda)_{\lambda'0} \right\}, \quad (4)$$

up to second order in the surface coordinate $\alpha_{\lambda\mu}$, where $R_T^{(0)}$ is the equivalent sharp surface radius of the target nucleus. In the collective model of surface oscillations, the surface coordinates $\alpha_{\lambda\mu}$ are treated as dynamical variables. They are related to the phonon creation and annihilation operators by

$$\alpha_{\lambda\mu} = \alpha_0 (a_{\lambda\mu}^\dagger + (-)^\mu a_{\lambda-\mu}), \quad (5)$$

where α_0 is the amplitude of the zero point motion. It is related to the deformation parameter β_λ by $\alpha_0 = \beta_\lambda / \sqrt{2\lambda+1}$ [31] and can be estimated from the measured transition probability using

$$\alpha_0 = \frac{1}{\sqrt{2\lambda+1}} \frac{4\pi}{3Z_T (R_T^{(0)})^\lambda} \sqrt{\frac{B(E\lambda)^\dagger}{e^2}}. \quad (6)$$

This equation is valid if the amplitude of the vibration is small and the transition operator is linearly proportional to α_0 .

The Coulomb components of the coupling form factors V_{nm} in Eq. (1) are obtained by taking the matrix elements of V_C between n - and m -phonon states. Since we assume that there exists only the one-phonon state in the vibrational excitation of the target, the Coulomb coupling form factors up to second order of α_0 are given by

$$V_{01}^{(C)}(r) = V_{10}^{(C)}(r) = \frac{3}{2\lambda+1} Z_P Z_T e^2 \frac{(R_T^{(0)})^\lambda}{r^{\lambda+1}} \sqrt{\frac{2\lambda+1}{4\pi}} \alpha_0, \quad (7)$$

$$V_{11}^{(C)}(r) = 2 \sum_{\lambda' \neq 0} (-)^{\lambda'} \frac{3(2\lambda+1)(\lambda'+2)}{8\pi(2\lambda'+1)} \\ \times \langle \lambda 0 \lambda 0 | \lambda' 0 \rangle^2 \alpha_0^2 Z_P Z_T e^2 \frac{(R_T^{(0)})^{\lambda'}}{r^{\lambda'+1}}. \quad (8)$$

If there exist two-phonon multiplets, then the formalism becomes much more complicated in the case of nonlinear coupling. In the case of the linear coupling, it is known that the no-Coriolis approximation enables us to replace the couplings to all the members of the two-phonon multiplets by the coupling to a single state by making an appropriate unitary transformation [14,28]. This leads to a significant reduction of the dimensions of the coupled channels problem. This property is lost if one keeps higher order terms of the Coulomb coupling since the radial dependence of the coupling form factor for the Coulomb part explicitly depends on the multipolarity of the nuclear excitation.

We now apply Eqs. (7) and (8) to fusion reactions between two ^{58}Ni nuclei, where the importance of second order couplings in the nuclear interaction has been reported [25]. We take into account the quadrupole vibrational state at 1.45 MeV, and truncate the whole space at the one-phonon state. The parameters for the nuclear potential and the deformation parameter from Ref. [25] have been used. Since at this stage we want to investigate the effects of higher order Coulomb coupling, a linear coupling for the nuclear interaction has been used, for ease of calculation. The coupled channels equations are solved by imposing the incoming wave boundary condition in the inner region of the fusion potential. We found that the second order coupling in the Coulomb interaction causes no visible effects to the fusion cross section. It changes the fusion cross section by only about 0.2% in the energy region we considered, i.e., from about 10 MeV below

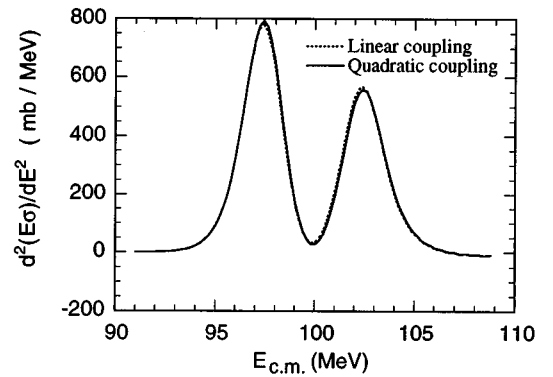


FIG. 1. The barrier distribution for fusion between two ^{58}Ni nuclei. The one-phonon state of the quadrupole surface vibration is taken into account. The nuclear interaction is treated in the linear coupling approximation. The dotted line corresponds to the case where the Coulomb coupling potential is also treated in the linear coupling approximation, while the solid line takes into account nonlinear terms up to second order.

the Coulomb barrier to about 10 MeV above the Coulomb barrier. Figure 1 shows the barrier distribution $[d^2(E_{c.m.}\sigma)/dE_{c.m.}^2]$ as a function of the bombarding energy. As seen from the figure, second order Coulomb couplings modify only very marginally the barrier distribution. Further calculations showed that the situation does not change when the value of the deformation parameter is varied within physically plausible limits. Therefore we hereafter use the linear coupling approximation for the Coulomb coupling and investigate the effects of the higher order terms only for nuclear coupling. The matrix elements of the Coulomb coupling form factor in Eq. (1) are now given by

$$V_{nm}^{(C)}(r) = \frac{3}{2\lambda+1} Z_P Z_T e^2 \frac{(R_T^{(0)})^\lambda}{r^{\lambda+1}} \sqrt{\frac{2\lambda+1}{4\pi}} \times \alpha_0 (\sqrt{n} \delta_{n,m+1} + \sqrt{n+1} \delta_{n,m-1}) \quad (9)$$

$$= \frac{3}{2\lambda+1} Z_P Z_T e^2 \frac{(R_T^{(0)})^\lambda}{r^{\lambda+1}} \frac{\beta_\lambda}{\sqrt{4\pi}} \times (\sqrt{n} \delta_{n,m+1} + \sqrt{n+1} \delta_{n,m-1}). \quad (10)$$

Note that we have defined the multiphonon channels by taking the appropriate linear combinations of the multiphonon multiplets. As remarked before, this is possible only for the linear coupling approximation in the Coulomb interaction.

B. Nuclear coupling form factors

In the collective model, the nuclear interaction is assumed to be a function of the separation distance between the vibrating surfaces of the colliding nuclei. It is conventionally taken as

$$V^{(N)}(r, \alpha_{\lambda 0}) = - \frac{V_0}{1 + \exp\{\{r - R_P - R_T^{(0)} - [\sqrt{(2\lambda+1)/4\pi}] R_T^{(0)} \alpha_{\lambda 0}\}/a\}}. \quad (11)$$

Volume conservation introduces a small term which is nonlinear with respect to the deformation parameter $\alpha_{\lambda 0}$ in the denominator of the above Eq. (11). This is ignored for simplicity in the present study. As in the case of Eq. (2) for the Coulomb coupling, here we consider the coupling form factor for the forward angle, which is needed to obtain the coupled channels equations in the no-Coriolis approximation. We assume a Woods-Saxon form for the nuclear potential. The structure of the resultant formulas in this subsection, however, remain unchanged for other forms of the nuclear potential. Denoting the eigenvalue of $\alpha_{\lambda 0}$ by x , the matrix elements of the nuclear coupling form factor read

$$V_{nm}^{(N)}(r) = \int_{-\infty}^{\infty} dx u_n^*(x) u_m(x) \frac{-V_0}{1 + \exp\{\{r - R_P - R_T^{(0)} - [\sqrt{(2\lambda+1)/4\pi}] R_T^{(0)} x\}/a\}}. \quad (12)$$

$u_n(x)$ is the eigenfunction of the n th excited state of the harmonic oscillator. The conventional nuclear coupling form factor in the linear coupling approximation is obtained by expanding Eq. (11) with respect to $\alpha_{\lambda 0}$ and keeping only the linear term.

The expectation value of the nuclear potential in the ground state is often replaced by the phenomenological potential

$$V_N(r) = - \frac{V_0}{1 + \exp[(r - R_P - R_T^{(0)})/a]}, \quad (13)$$

which is assumed to be known empirically [25]. If we take this prescription, the nuclear coupling form factor in Eq. (1) is calculated as

$$V_{nm}^{(N)}(r) = \int_{-\infty}^{\infty} dx u_n^*(x) u_m(x) \frac{-V_0}{1 + \exp\{\{r - R_P - R_T^{(0)} - [\sqrt{(2\lambda+1)/4\pi}] R_T^{(0)} x\}/a\}} - \delta_{n,m} \int_{-\infty}^{\infty} dx |u_0(x)|^2 \frac{-V_0}{1 + \exp\{\{r - R_P - R_T^{(0)} - [\sqrt{(2\lambda+1)/4\pi}] R_T^{(0)} x\}/a\}}. \quad (14)$$

The last term in this equation is included to make the coupling interaction vanish in the entrance channel. Equation (14) represents the form factor which contains couplings to all orders. We use these form factors in the next section in order to discuss the effects of higher order coupling to vibrational modes of excitation of the colliding nuclei on heavy-ion fusion reactions.

Instead of introducing a phenomenological potential given

by Eq. (13) as the bare potential in the entrance channel, one could use $V_{00}^{(N)}$ in Eq. (12) as the nuclear potential in the entrance channel. The use of Eq. (13) makes it easier to examine the convergence of the effects of higher order terms by comparing the results of the calculations in the linear and the quadratic approximations and the full order calculations. Notice that $V_{00}^{(N)}$ is identical with the potential given by Eq. (13) in the linear coupling approximation.

III. RESULTS: EFFECTS OF HIGHER ORDER COUPLINGS

A. Nearly symmetric systems

We now present the results of our calculations of fusion cross sections, average angular momenta of the compound nucleus, and fusion barrier distributions. We first discuss heavy, nearly symmetric systems. The experimental data of the average angular momentum of the compound nucleus for several systems are summarized in Fig. 5 of Ref. [17]. It suggests that the conventional coupled channels calculations do not work for heavy, nearly symmetric systems. We analyze in particular $^{64}\text{Ni} + ^{92,96}\text{Zr}$ reactions which are typical examples where the conventional coupled channels calculations with the linear coupling approximation fail to reproduce the fusion cross sections and average angular momentum data [21]. Our aim is to investigate whether the failure is due to the linear coupling approximation by performing linear, quadratic, and full coupling calculations.

We take into account the couplings up to two-phonon states of the quadrupole surface vibrations of ^{64}Ni and ^{92}Zr , and of the octupole vibration of ^{96}Zr . We also take their mutual excitations into account. We ignore the effects of transfer reactions, because it has been reported in Ref. [21] that they have only small effects on the fusion cross sections and the average angular momenta in these reactions. The excitation energies of the single-phonon states in ^{64}Ni , ^{92}Zr , and ^{96}Zr are 1.34, 0.934, and 1.897 MeV, respectively. We assumed the radius parameter associated with the coupling interactions to be 1.2 fm in all cases. The deformation parameter of ^{64}Ni was taken to be $\beta_2 = 0.19$ [25]. Following Refs. [14,32] we used $\beta_2 = 0.25$ for the nuclear coupling associated with the quadrupole vibration of ^{92}Zr , while the deformation parameter in the Coulomb coupling interaction was estimated from the measured $B(E2) \uparrow$ value to be 0.108. The different value for the nuclear deformation parameter from that of the Coulomb coupling parameter was required in order to fit the angular distribution of the inelastic scattering of ^{16}O from ^{92}Zr at 56 MeV [32]. The deformation parameter β_3 of ^{96}Zr was estimated from the recently measured $B(E3) \uparrow$ value [33] to be 0.268. We assumed the same value for the deformation parameter for the nuclear coupling as that for the Coulomb deformation parameter for this nucleus. The nuclear potentials used in this paper are the same as in Ref. [21]. These modify the empirical potentials of Christensen and Winther [34] by setting the range adjustment parameter ΔR to be 0 fm.

The excitation function of the fusion cross section for these two systems obtained by numerically solving the coupled channels equations is compared with the experimental data in Figs. 2 and 3 (upper panels). The experimental data, taken from Ref. [21], consist only of the evaporation residue cross sections, and do not include fission following fusion. The dotted lines are the results in the one-dimensional potential model, i.e., without the effects of channel coupling. As is well known, the experimental fusion cross sections at sub-barrier energies are several orders of magnitude larger than the predictions of this model. The dot-dashed lines are the results of the coupled channels calculations when the linear coupling approximation is used, which are similar to the results of the simplified coupled channels

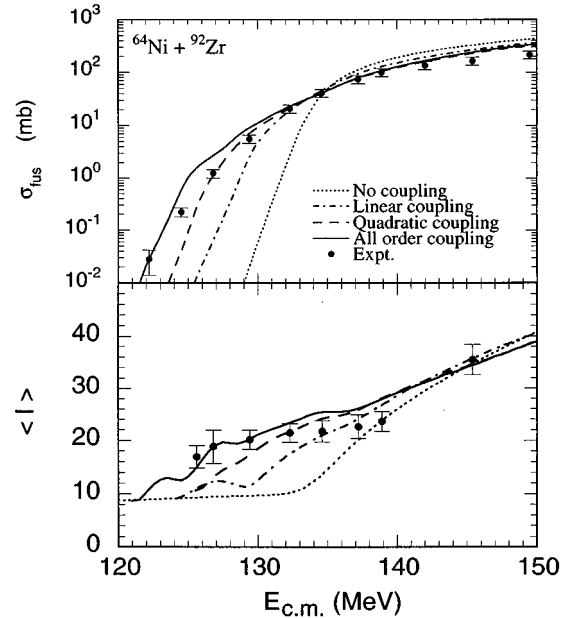


FIG. 2. Excitation function of the fusion cross section (upper panel) and the average angular momentum of the compound nucleus (lower panel) for the $^{64}\text{Ni} + ^{92}\text{Zr}$ reaction. The experimental data are taken from Ref. [21]. The two-phonon states of the quadrupole surface vibration of both the projectile and the target are taken into account in the coupled channels calculations. The dotted line is the result in the absence of channel coupling. The dot-dashed and the dashed lines are the results when the nuclear potential is expanded up to the first and the second order terms in the deformation parameters, respectively. The solid line is the results of the coupled channels calculations to all orders, obtained without expanding the nuclear potential.

calculations reported in Ref. [21]. They considerably underestimate the fusion cross sections at sub-barrier energies for both systems. The situation is slightly improved when the quadratic coupling approximation is used, i.e., when the nuclear coupling potential up to the second order of the deformation parameter [25] is included (dashed lines). However, there still remain considerable discrepancies between the experimental data and the results of the coupled channels calculations. When we include couplings to all order, we get the solid lines, which agree very well with the experimental data. Dramatic effects of the higher order couplings on fusion cross sections are observed, especially at low energies. The slight underestimate of the fusion cross section at 121.6 MeV in the $^{64}\text{Ni} + ^{96}\text{Zr}$ reaction will be improved by taking the effects of transfer reactions into account [35].

The lower panels in Figs. 2 and 3 compare the results of our calculations of the average angular momentum of the compound nucleus with the experimental data as a function of the bombarding energy. It is defined in terms of the partial fusion cross section σ_l as

$$\langle l \rangle = \frac{\sum_l l \sigma_l}{\sum_l \sigma_l}. \quad (15)$$

The meaning of each line in these figures is the same as in the upper panels. We again observe that the experimental data are much better reproduced by taking the effects of cou-

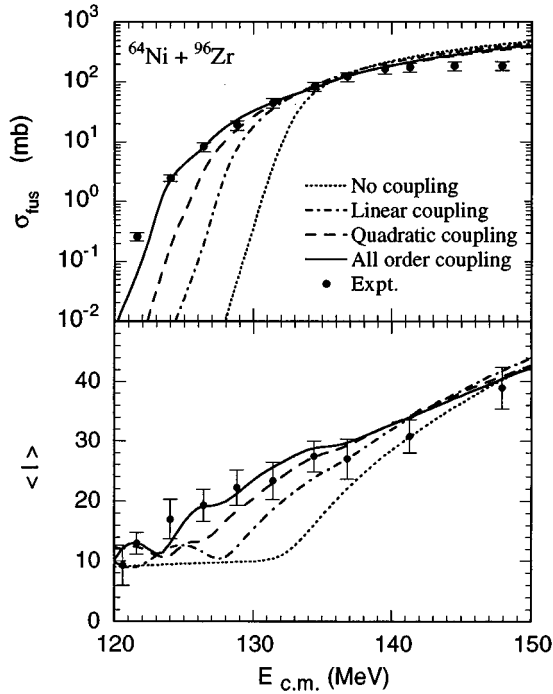


FIG. 3. Same as Fig. 2, but for $^{64}\text{Ni} + ^{96}\text{Zr}$ fusion. The two-phonon states of the quadrupole surface vibrations of the projectile and those of the octupole surface vibrations of the target are taken into account in the coupled channels calculations. The experimental data are taken from Ref. [21].

plings to all orders into account. We thus conclude that coupling to all orders is essential to simultaneously reproduce the fusion cross sections and the average angular momentum data for heavy (nearly) symmetric systems. This is in agreement with the calculations required to fit the barrier distribution for the $^{58}\text{Ni} + ^{60}\text{Ni}$ reaction [7].

B. Very asymmetric systems

We next consider the effects of higher order couplings for very asymmetric systems where the product of the charges $Z_P Z_T$ is relatively small. For such systems, the coupled channels calculations in the linear coupling approximation have achieved reasonable success in reproducing fusion excitation functions. However, no study has been performed to see whether the effects of higher order couplings on the angular momentum distribution of the compound nucleus and on the barrier distributions are small. In this subsection we reanalyze the experimental data for the $^{16}\text{O} + ^{112}\text{Cd}$ reaction, for which both fusion cross sections and average angular momentum data are available [22], and those for the $^{16}\text{O} + ^{144}\text{Sm}$ reaction, where the fusion barrier distribution has been extracted from the precisely measured fusion cross sections [6]. For simplicity in the calculations we ignore excitation of the projectile in both reactions. These effects will be discussed in a separate paper [36], where it will be shown that the octupole vibration of ^{16}O leads to a static renormalization of the fusion barrier [37,38].

In calculating the fusion cross section for $^{16}\text{O} + ^{112}\text{Cd}$ scattering, we include the double quadrupole phonon states and the single octupole phonon state of ^{112}Cd and their mu-

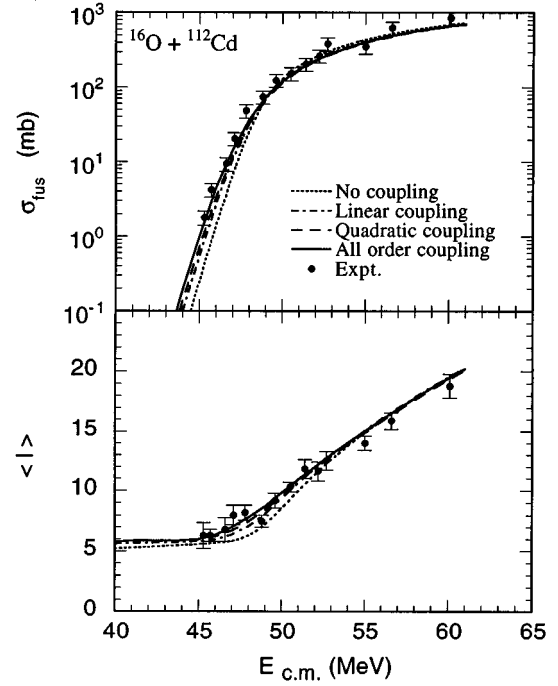


FIG. 4. Same as Fig. 2, but for $^{16}\text{O} + ^{112}\text{Cd}$ fusion. In the coupled channels calculations, the projectile is assumed to be inert. The one- and two-phonon quadrupole states and the one-phonon octupole state of the target are taken into account. The experimental data are taken from Ref. [22].

tual excitations. The excitation energies are 0.617 and 2.005 MeV for the one-phonon states of the quadrupole and the octupole vibrations, respectively. The deformation parameters of the quadrupole and the octupole vibrations are estimated to be $\beta_2 = 0.173$ and $\beta_3 = 0.164$, respectively [22]. The radius parameter in the coupling interaction is taken to be 1.2 fm. Following Ref. [22], we use a Woods-Saxon potential whose depth, range parameter, and surface diffuseness are $V = 58$ MeV, $r_0 = 1.22$ fm, and $a = 0.63$ fm, respectively.

The upper panel of Fig. 4 compares the results of the coupled channels calculations of fusion cross sections with the experimental data taken from Ref. [22]. Compared with the symmetric systems studied in the previous subsection, the enhancement of the fusion cross sections is fairly small. This is partly because the product of the atomic number $Z_P Z_T$ in this asymmetric system is smaller than the symmetric systems. If we take the linear coupling approximation and estimate the coupling strength F at the barrier position r_B of the bare Coulomb barrier, we find

$$F = \frac{\beta_\lambda}{\sqrt{4\pi}} Z_P Z_T e^2 \left(-\frac{R_T^{(0)}}{r_B^2} + \frac{3}{2\lambda+1} \frac{(R_T^{(0)})^\lambda}{r_B^{\lambda+1}} \right). \quad (16)$$

The coupling strength is thus proportional to the product $Z_P Z_T$. This product is 384 for $^{16}\text{O} + ^{112}\text{Cd}$ scattering, while it is 1120 for $^{64}\text{Ni} + ^{92,96}\text{Zr}$ reactions. The coupling strength in this asymmetric system is therefore several times smaller than in the symmetric systems, even though the values of the deformation parameters are similar. Another reason that the enhancement of the fusion cross sections is small in very asymmetric systems is the small reduced mass. In the WKB

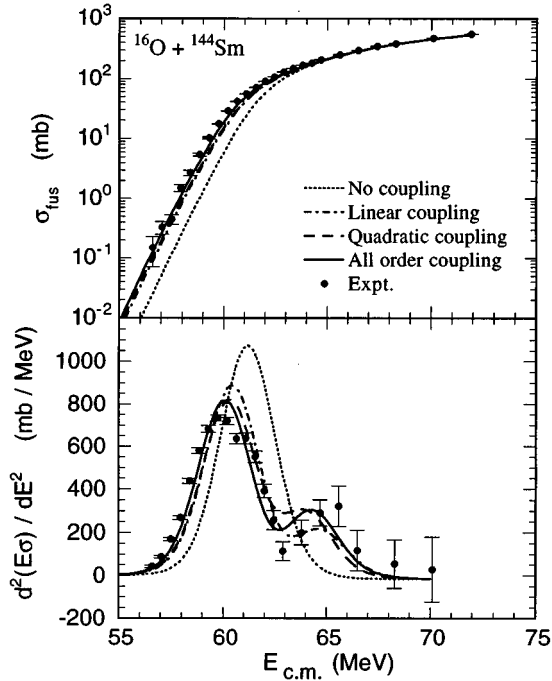


FIG. 5. Excitation function of the fusion cross section (upper panel) and the barrier distribution (lower panel) for $^{16}\text{O} + ^{144}\text{Sm}$ fusion. In the coupled channels calculations, the projectile is assumed to be inert, while the single octupole phonon state of the target is taken into account. The meaning of each line is the same as in Fig. 2. The experimental data are taken from Ref. [6].

formula for the barrier penetrability, the mass parameter appears in the exponent. Hence the heavier the mass, the more sensitive the penetrability to a slight change of the potential. Even though the results in the linear coupling approximation (dot-dashed line) show a relatively small enhancement of the fusion cross section compared with the no-coupling limit, there is still a significant change in going to second order coupling, and then to all order coupling. The situation is similar for the average angular momentum. Thus even in such cases with low $Z_p Z_T$, if data of high precision are available, it seems that the linear coupling approximation is inadequate to allow quantitative conclusions to be drawn from a comparison of data and calculations.

The role of higher order couplings in very asymmetric systems can be more clearly seen by investigating the fusion barrier distributions. Therefore, we next consider the $^{16}\text{O} + ^{144}\text{Sm}$ reaction, for which the effects on fusion barrier distributions of couplings to phonon states were shown experimentally for the first time [5,6,11]. The authors of Ref. [6] have shown that the fusion barrier distribution for this system is intimately related to the octupole vibration of ^{144}Sm , and that the quadrupole vibration plays only a minor role. Accordingly, we ignore the effects of the couplings to the quadrupole phonon states of ^{144}Sm and include only the single octupole phonon state at 1.81 MeV. The deformation parameter $\beta_3 = 0.205$ was used as in Ref. [6]. The ion-ion potential was of a Woods-Saxon form. The depth, radius parameter, and surface diffuseness were 105.1 MeV, 1.1 fm, and 0.75 fm, respectively, as given in Ref. [39].

The upper panel of Fig. 5 shows the fusion excitation function from Ref. [6], and the calculations. The meaning of

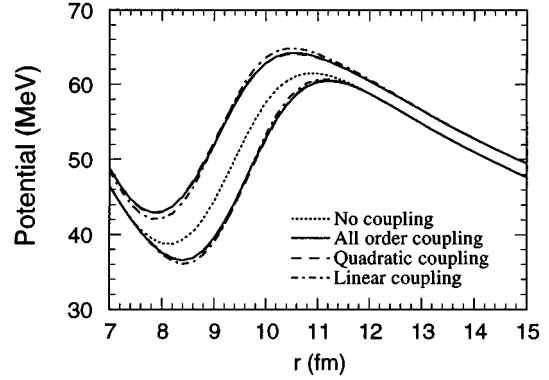


FIG. 6. Effective potential barriers for the s -wave scattering of ^{16}O from ^{144}Sm obtained by diagonalizing the coupling matrix. The meaning of each line is the same as in Fig. 5.

each line is the same as in Fig. 2. As was the case for $^{16}\text{O} + ^{112}\text{Cd}$, we observe that the agreement of the theory and experiment appears to be improved only slightly by the inclusion of coupling to all orders. The barrier distribution, however, reveals significant changes due to the higher order couplings (see the lower panel of Fig. 5). Note that there exist two barriers in the present two-channel problem. Comparing the results of the linear coupling approximation (the dot-dashed line) with those of the all order coupling (the solid line), one observes that the higher order couplings transfer some strength from the lower barrier to the higher barrier, and at the same time lower the energies of both barriers.

This can be viewed in a different way by performing the diagonalization of the coupling matrix at each position of the internuclear separation to obtain the effective barriers, as is done in the computer code CCMOD [23]. Figure 6 shows these effective barriers for s -wave scattering. The meaning of each line is the same as in Fig. 5. We observe that higher order couplings decrease the energies of both the lower and the higher barriers, consistent with the barrier distributions shown in Fig. 5. The higher order couplings also increase the width of both potential barriers (Fig. 6), leading to narrower peaks in the barrier distribution. This then results in the apparent better separation between the two barriers seen in Fig. 5.

For these asymmetric reactions, the couplings are weak as a result of a combination of the small product of $Z_p Z_T$ and the relatively small deformation parameters. In such cases the first order approximation might have been expected to be valid. Despite this, the calculations which include couplings to all orders show significant differences from first order calculations. It is clear therefore that high precision measurements should be analyzed using all order couplings even when coupling is weak.

IV. SUMMARY

We have shown that in heavy-ion fusion reactions, higher order couplings to nuclear surface vibrations play an important role. Such higher order terms in the Coulomb coupling can be safely neglected. Previous work indicated that standard coupled channels calculations are not very successful in describing the fusion of heavy symmetric systems. We have

shown that the data can be described well by coupled channels calculations once couplings to all orders are included. We found that for the $^{64}\text{Ni} + ^{92,96}\text{Zr}$ reactions, terms beyond those in the quadratic coupling approximation result in further enhancement of the fusion cross sections at sub-barrier energies. The additional enhancement is as large as that due to the inclusion of quadratic coupling. The inclusion of the coupling to all orders is crucial to reproduce the experimental fusion cross sections and the average angular momenta. We performed calculations also for the $^{16}\text{O} + ^{112}\text{Cd}$, ^{144}Sm reactions as examples of very asymmetric systems where the coupling is weaker. It is found that in such cases higher order couplings result in a non-negligible enhancement of the fusion cross sections and a significant modification of barrier distributions as well as the average angular momenta.

High precision fusion cross section measurements to deduce the barrier distribution and measurements of angular momentum distributions are designed to study the important couplings in a reaction. The sensitivity to couplings is greatly enhanced by performing experiments involving target projectile combinations with a large value of $Z_p Z_T$. It has been shown in this paper that higher order coupling significantly affects the barrier distribution and average angular

momentum even for weak coupling cases like $^{16}\text{O} + ^{112}\text{Cd}$, ^{144}Sm with values of $Z_p Z_T \sim 400$. Thus, spurious conclusions regarding the nature of couplings could be reached if high quality experimental data, particularly for heavier systems, are compared with calculations performed only with first order coupling. The stage has now been reached when the standard codes of the coupled channels calculations should be revised to include coupling to all orders.

ACKNOWLEDGMENTS

The authors thank S. Kuyucak, J. R. Bennett, I. J. Thompson, and M. Abe for useful discussions. K.H. and N.T. also thank the Australian National University for its hospitality and for partial support for this project. The work of K.H. was supported by the Japan Society for the Promotion of Science for Young Scientists. This work was supported by the Grant-in-Aid for General Scientific Research, Contract Nos. 06640368 and 08640380, and a Grant-in-Aid for Scientific Research on Priority Areas, Contracts Nos. 05243102 and 08240204 from the Japanese Ministry of Education, Science and Culture, and a bilateral program of JSPS between Japan and Australia.

-
- [1] N. Rowley, G.R. Satchler, and P.H. Stelson, *Phys. Lett. B* **254**, 25 (1991).
- [2] J.X. Wei, J.R. Leigh, D.J. Hinde, J.O. Newton, R.C. Lemmon, S. Elfstrom, J.X. Chen, and N. Rowley, *Phys. Rev. Lett.* **67**, 3368 (1991).
- [3] R.C. Lemmon, J.R. Leigh, J.X. Wei, C.R. Morton, D.J. Hinde, J.O. Newton, J.C. Mein, M. Dasgupta, and N. Rowley, *Phys. Lett. B* **316**, 32 (1993).
- [4] J.R. Leigh, N. Rowley, R.C. Lemmon, D.J. Hinde, J.O. Newton, J.X. Wei, J.C. Mein, C.R. Morton, S. Kuyucak, and A.T. Kruppa, *Phys. Rev. C* **47**, R437 (1993).
- [5] C.R. Morton, M. Dasgupta, D.J. Hinde, J.R. Leigh, R.C. Lemmon, J.P. Lestone, J.C. Mein, J.O. Newton, H. Timmers, N. Rowley, and A.T. Kruppa, *Phys. Rev. Lett.* **72**, 4074 (1994).
- [6] J.R. Leigh, M. Dasgupta, D.J. Hinde, J.C. Mein, C.R. Morton, R.C. Lemmon, J.P. Lestone, J.O. Newton, H. Timmers, J.X. Wei, and N. Rowley, *Phys. Rev. C* **52**, 3151 (1995).
- [7] A.M. Stefanini, D. Ackermann, L. Corradi, D.R. Napoli, C. Petrache, P. Spolaore, P. Bednarczyk, H.Q. Zhang, S. Beghini, G. Montagnoli, L. Mueller, F. Scarlassara, G.F. Segato, F. Sorame, and N. Rowley, *Phys. Rev. Lett.* **74**, 864 (1995).
- [8] A.M. Stefanini, D. Ackermann, L. Corradi, J.H. He, G. Montagnoli, S. Beghini, F. Scarlassara, and G.F. Segato, *Phys. Rev. C* **52**, R1727 (1995).
- [9] J.D. Bierman, P. Chan, J.F. Liang, M.P. Kelly, A.A. Sonzogni, and R. Vandenbosch, *Phys. Rev. Lett.* **76**, 1587 (1996).
- [10] D.J. Hinde, M. Dasgupta, J.R. Leigh, J.C. Mein, C.R. Morton, J.O. Newton, and H. Timmers, *Phys. Rev. C* **53**, 1290 (1996).
- [11] N. Rowley, H. Timmers, J.R. Leigh, M. Dasgupta, D.J. Hinde, J.C. Mein, C.R. Morton, and J.O. Newton, *Phys. Lett. B* **373**, 23 (1996).
- [12] M. Beckerman, *Rep. Prog. Phys.* **51**, 1047 (1988).
- [13] K. Hagino, N. Takigawa, J.R. Bennett, and D.M. Brink, *Phys. Rev. C* **51**, 3190 (1995).
- [14] A.T. Kruppa, P. Romain, M.A. Nagarajan, and N. Rowley, *Nucl. Phys.* **A560**, 845 (1993).
- [15] R. Vandenbosch, *Annu. Rev. Nucl. Sci.* **42**, 447 (1992), and references therein.
- [16] A. Charlop, J. Bierman, Z. Drebi, A. García, D. Prindle, A.A. Sonzogni, R. Vandenbosch, D. Ye, S. Gil, F. Hasenbalg, J.E. Testoni, D. Abriola, M. di Tada, A. Etchegoyen, M.C. Berisso, J.O. Fernández-Niello, and A.J. Pacheco, *Phys. Rev. C* **49**, R1235 (1994).
- [17] A. Charlop, J. Bierman, Z. Drebi, A. García, S. Gil, D. Prindle, A. Sonzogni, R. Vandenbosch, and D. Ye, *Phys. Rev. C* **51**, 628 (1995).
- [18] N. Rowley, J.R. Leigh, J.X. Wei, and R. Lindsay, *Phys. Lett. B* **314**, 179 (1993).
- [19] A.B. Balantekin, J.R. Bennett, and S. Kuyucak, *Phys. Lett. B* **335**, 295 (1994).
- [20] K.E. Rehm, H. Esbensen, J. Gehring, B. Glagola, D. Henderson, W. Kutschera, M. Paul, F. Soramel, and A.H. Wuosmaa, *Phys. Lett. B* **317**, 31 (1993).
- [21] A.M. Stefanini, L. Corradi, D. Ackermann, A. Facco, F. Gramegna, H. Moreno, L. Mueller, D.R. Napoli, G.F. Prete, P. Spolaore, S. Beghini, D. Fabris, G. Montagnoli, G. Nebbia, J.A. Ruiz, G.F. Segato, C. Signorini, and G. Viesti, *Nucl. Phys.* **A548**, 453 (1992).
- [22] D. Ackermann, L. Corradi, D.R. Napoli, C.M. Petrache, P. Spolaore, A.M. Stefanini, F. Scarlassara, S. Beghini, G. Montagnoli, G.F. Segato, and C. Signorini, *Nucl. Phys.* **A575**, 374 (1994).
- [23] M. Dasgupta, A. Navin, Y.K. Agarwal, C.V.K. Baba, H.C. Jain, M.L. Jhingan, and A. Roy, *Nucl. Phys.* **A539**, 351 (1992).
- [24] A.B. Balantekin, J.R. Bennett, and S. Kuyucak, *Phys. Rev. C* **48**, 1269 (1993); **49**, 1079 (1994).
- [25] H. Esbensen and S. Landowne, *Phys. Rev. C* **35**, 2090 (1987).

- [26] N. Rowley, in *Proceedings of the International Workshop on Heavy-Ion Fusion: Exploring the Variety of Nuclear Properties*, edited by A.M. Stefanini *et al.* (World Scientific, Singapore, 1994), p. 66.
- [27] V. Yu. Denisov and G. Royer, *Phys. At. Nuclei* **58**, 397 (1995); *J. Phys. G* **20**, L43 (1994).
- [28] N. Takigawa and K. Ikeda, in *Proceedings of the Symposium on Many Facets of Heavy Ion Fusion Reactions*, edited by W. Henning *et al.* (Argonne National Laboratory Report No. ANL-PHY-87-1, 1986), p. 613.
- [29] K. Hagino, N. Takigawa, A.B. Balantekin, and J.R. Bennett, *Phys. Rev. C* **52**, 286 (1995).
- [30] P. Ring and P. Schuck, *The Nuclear Many Body Problem* (Springer-Verlag, New York, 1980).
- [31] A. Bohr and B.R. Mottelson, *Nuclear Structure* (Benjamin, Reading, MA, 1975), Vol. 2.
- [32] E.M. Takagui, G.R. Satchler, H. Takai, K. Koide, and O. Dietzsch, *Nucl. Phys.* **A514**, 120 (1990).
- [33] D.J. Horen, R.L. Auble, G.R. Satchler, J.R. Beene, I.Y. Lee, C.Y. Wu, D. Cline, M. Devlin, R. Ibbotson, and M.W. Simon, *Phys. Rev. C* **48**, R2131 (1993).
- [34] P.R. Christensen and A. Winther, *Phys. Lett.* **65B**, 19 (1976).
- [35] H. Esbensen and S. Landowne, *Nucl. Phys.* **A492**, 473 (1989).
- [36] K. Hagino, N. Takigawa, M. Dasgupta, D.J. Hinde, and J.R. Leigh (unpublished).
- [37] N. Takigawa, K. Hagino, M. Abe, and A.B. Balantekin, *Phys. Rev. C* **49**, 2630 (1994).
- [38] N. Takigawa, K. Hagino, and M. Abe, *Phys. Rev. C* **51**, 187 (1995).
- [39] C.R. Morton, Ph.D. thesis, the Australian National University, 1995.